Precise Measurements of the Storage Lifetimes of Highly Charged Heavy Ions in the CSRe Storage Ring using a Schottky Resonator*

Qian Wang,[1,†] Xin-Liang Yan,[1,2,‡] Guang-Yu Zhu,[1] Shahab Sanjari,[3,4] Li-Jun Mao,[1,2] He Zhao,[1,2] Yuri A. Litvinov,[3] Rui-Jiu Chen,[3] Meng Wang,[1,2,§] Yu-Hu Zhang,[1,2] You-Jin Yuan,[1,2] Jun-Xia Wu,[1,2] Hong-Yang Jiao,[1,2] Yue Yu,[1,2] Zu-Yi Chen,[1,2] and Yin-Fang Luo[1,2]

[1]*Institute of Modern Physics, Chinese Academy of Sciences, Lanzhou 730000, China*
[2]*University of Chinese Academy of Sciences, Beijing 100049, China*
[3]*GSI Helmholtzzentrum für Schwerionenforschung, Planckstrasse 1, Darmstadt 64291, Germany*
[4]*FH Aachen University of Applied Sciences, Heinrich-Mussmann-Str. 1, Jülich 52428, Germany*

Schottky mass spectrometry utilizing heavy-ion storage rings serves as a powerful technique for precision mass and decay half-life measurements of highly charged ions. The number of stored ions in the ring is determined by the peak area in the revolution frequency spectrum. Due to intrinsic amplitude frequency characteristic (AFC), Schottky detector systems exhibit varying sensitivities at different frequencies. In this paper, a new method was developed in order to calibrate the AFC curve of the Schottky detector system of the CSRe storage ring using low-energy electron-cooled stored ions. With the amplitude-calibrated frequency spectrum, there was a notable refinement in the precision of both the peak position and peak area. As a result, the storage lifetimes of the electron-cooled fully-ionized $^{56}Fe^{26+}$ ions were determined with high precision at the beam energy of 13.7 MeV/u and 116.4 MeV/u, despite of frequency drifts during the experiment. When the electron cooling is turned off, the effective vacuum condition experienced by the 116.4 MeV/u $^{56}Fe^{26+}$ ions was determined using the amplitude-calibrated spectra, revealing a value of 10^{-10} mbar which is consistent with the vacuum gauges readings along the CSRe ring. The method reported here can be adapted at other storage ring facilities to improve the precision and enhance the capability of life-time measurement in the ring.

Keywords: Lifetime Measurement, Schottky mass Spectrometry, Sensitivity response, Highly Charged Heavy Ion, Resonator, UH Vacuum, Non-destructive diagnostics

I. INTRODUCTION

The mass and lifetime are basic properties of atomic nuclei. To date, about 3400 nuclides have been identified, among which less than 300 are stable nuclei concerning radioactive decay [1]. Theoretical predictions indicate the potential existence of numerous additional particle-bound nuclei [2, 3]. Discovery of new isotopes and measurement of their mass and decay characterises needs powerful radioactive ion-beam facilities and fast sensitive detection techniques [4]. Utilizing heavy-ion storage rings coupled to radioactive beam lines, the time-resolved Schottky mass spectrometry provides a powerful tool for measuring the radioactive decay of highly charged ions and investigating exotic decay modes [5, 6].

In a storage ring, ion species are distinguished by their revolution frequencies, which correspond to their mass-to-charge ratios. This is a foundational principle of the storage ring mass spectrometry. The storage ring's high mass resolving power can be enhanced using an electron-cooling device and/or a ring designed for an isochronous ion-optical configuration [7]. These features make it possible to clearly identify particles in the measured frequency spectrum, which is crucial when the nuclei of interest were among a vast number of other ion species stored in the ring at the same time.

In the time-resolved Schottky mass spectrometry technique, the frequency spectra were continuously measured. The peak area of the revolution frequency in the spectra is proportional to the signal power induced in the Schottky detector by the corresponding ions [8]. By observing the reduction in peak area, the decline in ion numbers as a function of storage time can be monitored and the decay halflife can be deduced [5]. Traditionally, a capacitive Schottky detectors of the parallel plate type is used to detect electromagnetic signals induced by the passing ions [9, 10]. However, these detectors often exhibit low sensitivity, limiting their use in detecting low-yield, low charge-states ions. Higher sensitivity can be achieved using a resonant cavity [8, 11–13]. The main advantage of using resonant cavities as Schottky pick-ups is the increased sensitivity at the characteristic resonance frequency of the cavity. This enhancement makes them suitable devices for fast detection of low yield exotic isotopes even down to single ions [14]. Moreover, there is an added benefit from the higher resolution obtained at higher frequencies [11, 13]. Such detectors are presently operational at GSI-ESR (Germany) [15], RIKEN-R3 (Japan) [16], and HIRFL-CSRe (China) [17] storage rings and are being used to directly monitor the decay from parent to daughter nuclei [14].

The sensitivity of a Schottky detector system varies with frequency, which can be characterized by the amplitude-frequency characteristic (AFC) curve. Compared to parallel plates detector, the cavity resonator detector has an enhanced signal from ions as well as elevated background noise

* Supported by the Regional Development Youth Program of the Chinese Academy of Sciences (People's Character [2023] No. 15), Chinese Academy of Sciences Stable Support for Young Teams in Basic Research (YSBR-002), National Key R&D Program of China (2018YFA0404401) and Special Fund for Strategic Pilot Technology of Chinese Academy of Sciences (XDB34000000).
† Corresponding author, wangqian2016@impcas.ac.cn
‡ Corresponding author, yanxinliang08@impcas.ac.cn
§ Corresponding author, wangm@impcas.ac.cn

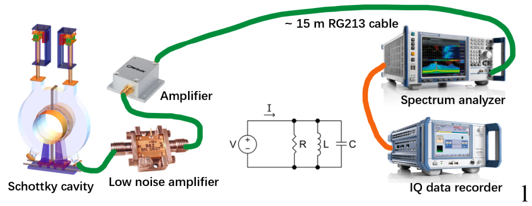

Fig. 1. Schematic illustration of the resonator Schottky detector system and its corresponding equivalent RLC circuit. The ion signal is captured by the Schottky cavity, amplified by a low-noise amplifier (LNA), filtered by a band-pass filter, and further amplified before being transmitted to the frequency analyzer via a 15-meter coaxial cable. The signal is then digitized by the spectrum analyzer and stored by the IQ data recorder.

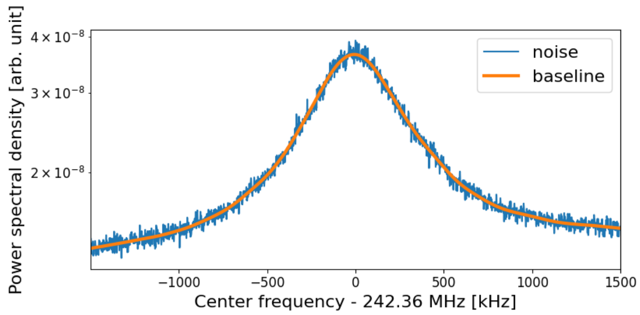

Fig. 2. Blue histogram: the measured thermal noise in the frequency domain when there is no beam in the CSRe. It can be used as a reference baseline in the subsequent measurement to extract the signal power induced by the storied ions. Orange line: the estimated baseline determined using the method of [18]. The reference level is set to -50 dBm, data acquisition time is 852.5 ms, frequency resolution is 0.92kHz, DAQ sampling rate is 3.75 MSamples/s.

level near the resonance frequency. This increased sensitivity results in a more pronounced sensitivity change across the same frequency span. In many-ion decay half-life measurement experiments, if the signal peak of a certain ion species is spread over wide frequency range due to a large momentum spread, or if the peak position shifts because of ongoing energy loss or beam manipulation using an electron-cooling device during the storage time, then calibration of the peak area is necessary before the corresponding particle count can be accurately determined.

In this work, a new method was developed in order to calibrate the sensitivity curve (AFC curve) of the Schottky detection system installed in the CSRe storage ring. This method, combined with the background noise subtraction technique, developed in our previous paper [18], has enabled a precise determination of storage lifetime of stable $^{56}Fe^{26+}$ ions in the ring. Once the revolution frequency spectra were normalized with the AFC curve, we were able to restore the peak shape and determine the peak center with better precision using Gaussian fitting. When the electron-cooling system was turned off, the ion beam gradually lost energy. By tracking the rate of change of the central frequency of the beam, we were able to determine the effective vacuum level experienced by the stored ions in the storage ring. The methodology developed in this paper can be adapted by other heavy-ion storage ring facilities for precision mass and lifetime measurements.

II. TIME-RESOLVED SCHOTTKY MASS SPECTROMETRY AT HEAVY-ION STORAGE RING

The scheme of the Schottky detection system is shown in Fig. 1. As ions pass through the cavity, they induce image charges and deposit energy, creating Schottky noise. This noise was extracted from the cavity using magnetic couplers [11], amplified by a low-noise amplifier (LNA) before finally been recorded by the spectrum analyzer. The measured data were analyzed online or offline revealing peaks at the ions' revolution frequency at each harmonics in the frequency domain (hereafter refer to as frequency spectrum) obtained using Fourier transformation.

A. The reference baseline in the measured frequency spectrum

Within the bandwidth of the detection system, the measured noise power includes both signal power, $P_{ion}(f)$, from the circulating ions in the ring and the thermal noise power, $P_{thermal}(f)$, of the detection system:

$$P_{total}(f) = P_{thermal}(f) + P_{ion}(f). \tag{1}$$

Due to the resonant nature of the cavity, the thermal noise exhibits a Lorentzian-like distribution in the frequency domain. Experimentally, power density profile of the thermal noise in the frequency domain can be measured when the beam is off. The result of the averaged spectrum can be served as a benchmark of the reference baseline (see the blue histogram in Fig.2) and subtracted from the frequency spectrum measured when the beam is present. Alternatively, the baseline can be estimated using the method described in Ref. [18], see the orange line shown in Fig.2 and in Fig.3. The advantage of this method is that baseline measurement can be done *in situ* when the beam is present and a smooth reference baseline can be obtained.

B. Information on the stored ions extracted from frequency peaks

After subtracting the thermal noise baseline, the remaining spectral components in the frequency spectrum are attributed to the periodic motion of the ions. Throughout the paper we consider only the case of coasting (i.e. not bunched) ion beam.

The Schottky noise originating from individual ions circulating in the ring at a specific revolution frequency f_{rev}, manifests as a series of distinct peaks in the frequency spectrum, each corresponding to different harmonic numbers $h = 1, 2, 3, \ldots$. The power density of each harmonic can be expressed as [5]:

$$\frac{\mathrm{d}P_{ion}(f)}{\mathrm{d}f} = 2q^2e^2\sum_{h=1}^{+\infty}\frac{f^2}{h^3}|H(f)|^2\xi(f), \tag{2}$$

where $|H(f)|$ represents the AFC function of the Schottky detector system, $\xi(f)$ is the normalized revolution frequency distribution of the ions and q is the electric charge of the ions. With h being the harmonic number, integration of the power density spectrum near a certain harmonic frequency hf_{rev}, results in

$$P_{ion} = \int_{hf_{rev}-\delta}^{hf_{rev}+\delta}\frac{\mathrm{d}P_{ion}}{\mathrm{d}f}\mathrm{d}f = 2N\left[|H(hf_{rev})|qef_{rev}\right]^2, \tag{3}$$

where N is the number of ions of a specific ion species. The value of δ is typically set to five standard deviations of the corresponding frequency peak hf_{rev}. The second equality in Eq. 3 holds true on the condition that the frequency spread of each ion remains sufficiently small during the measurement period.

For single-ion decay measurement experiments in heavy-ion storage ring, the decay event is determined unambiguously by the disappearance of the parent ion and the appearance of the daughter ion [14]. For other cases, by measuring the peak area in the frequency spectrum associated with an ion species of interest and by monitoring its evolution as a function of time, the fluctuation of the ion number can be monitored. In order to do that, the calibration of the AFC function of the detection system is important. Determination of the AFC function relies in principle on the fact that the measured signal peak areas that correspond to the same stored ion species in the ring remain consistent at any revolution frequency harmonics hf_{rev}.

III. CALIBRATION OF THE AFC FUNCTION

The resonant Schottky cavity detector installed in the CSRe has a pillbox design as shown in Fig. 1. Due to the characteristics of the equivalent RLC circuit , a similar AFC form as the one of the cavity [8, 11, 19, 20] was used for modeling the AFC function of the detector system:

$$|H(f)| = \frac{R_{sys}\gamma\sqrt{\zeta}}{\sqrt{1+Q_{sys}^2\left(\frac{f}{f_{sys}}-\frac{f_{sys}}{f}\right)^2}}, \tag{4}$$

where R_{sys} represents the resistance of the entire system's equivalent RLC circuit, ζ is the loss factor quantifying the energy loss to wake-fields [21], and γ is the relativistic Lorentz factor of the ions. Additionally, Q_{sys} and f_{sys} are the effective quality factor and the resonant frequency of the system, respectively. The AFC curve of the Schottky cavity can be measured offline utilizing a network analyzer. In contrast, determining the AFC curve for the entire detection system necessitates online beam experiments. The resulting AFC curve is influenced not only by the AFCs of the cavity, electronic components, and cables but also incorporates the AFC of the spectrum analyzer. The system's AFC can be ascertained by leveraging the feature of multiple-peaks of the same ion species appeared simultaneously at several frequency harmonics. If we are able to simultaneously measure at least two frequency harmonics of the same ion species in the spectrum, we could determine the relative sensitivity ratio between two different harmonic frequencies within the same spectrum.

The optimal method for measuring the AFC curve employs electron-cooled low-energy beams. The low ion energy leads to small frequency intervals between adjacent harmonics. Electron cooling is essential in order to ensure that the ion peak is narrow enough, so that the corresponding AFC region under it can be considered as constant.

As a result, multiple revolution frequency harmonics can be detected simultaneously within frequency range of the data acquisition (DAQ) system. By adjusting the electron cooler voltage, we can shift the center frequencies in steps to collect more data points along the AFC curve, thereby enabling us to determine the entire curve within the measured frequency range.

A. The calibration measurement

In the experiment, the electron-cooled $^{56}\mathrm{Fe}^{26+}$ ions at an energy of 13.6 MeV/u was utilized to measure the AFC curve within the 3 MHz bandwidth around the resonant frequency of the Schottky detector system . The measured time-resolved frequency spectrum is shown at Fig. 3. Up to 6 harmonics of the revolution frequency were covered. By adjusting the voltage of the electron cooler from 126.6 kV to 129.8 kV, the velocity of ions was altered in 13 increments. Consequently, the center frequencies of each harmonic were shifted by approximately 600 kHz in total.

As the number of the stored ions reduces due to inevitable particle losses as $N = N_0e^{-\lambda_t t}$, the integrated power decreases as a function of time:

$$P(t) = P_0e^{-\lambda_t t}, \tag{5}$$

where λ_t is the decay constant, $P_0 = 2N_0\left[|H(hf_{rev})|qef_{rev}\right]^2$, and N_0 is the initial number of ions. Based on Eq. (3)-(5), the integrated power of the ion beam at each harmonic in the spectrum can be expressed as a function of the center frequency of the harmonic $f = hf_{rev}$ and time t, denoted as

$$P(f,t|A_0,\lambda_t,Q_{sys},f_{sys}) = \frac{A_0}{1+Q_{sys}^2\left(\frac{f}{f_{sys}}-\frac{f_{sys}}{f}\right)^2}e^{-\lambda_t t}, \tag{6}$$

where $A_0 = 2N_0\zeta\left(R_{sys}\gamma qef_{rev}\right)^2$ is the initial peak area. The parameters A_0 and λ_t are related to the properties of ion beam, whereas Q_{sys} and f_{sys} are uniquely associated with the attributes of the detector system.

The specific data processing steps are as follows:

1. Estimate the reference baseline and subtract it to generate the background-free spectrum using the method described in Ref. [18]. See Fig. 3.

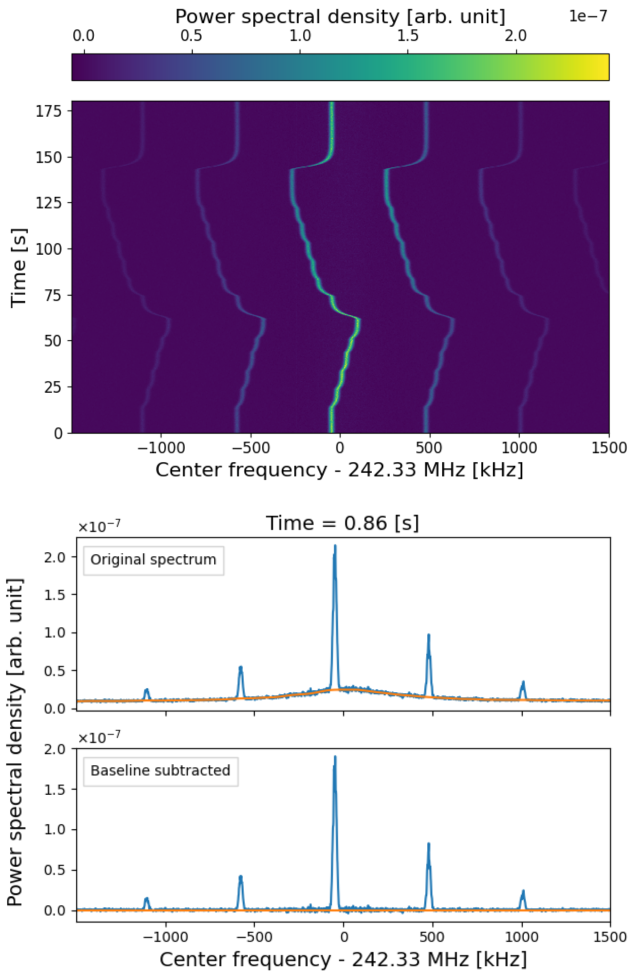

Fig. 3. Top:Time-resolved Schottky spectrum of electron-cooled $^{56}Fe^{26+}$ beam at an energy of 13.6 MeV/u. The velocity of the ions was shifted in steps such that the revolution frequency change covers the whole measurement frequency range of 3 MHz. The time resolution is 86 ms/channel and the frequency resolution is 0.92 kHz/channel. Middle: Single frame from the top panel at time = 0.86 seconds, including 5 harmonics $h = 614, 615, ..., 618$. The blue line indicates the original power density of the spectrum. The orange line is the estimated baseline [18]. Bottom: The same Spectrum as the frame in middle frame after baseline was subtracted.

2. For each spectrum at time t_j ($j = 1, 2, ..., n$), the peak area is calculated by simple integration for each peak at different harmonics. Here n is the number of bins in time during the continue spectrum recording process. This yields the experimental value $P^{exp}_{i,j}$ at frequency $f = f_i$ ($i = 1, ..., 6$ harmonic) and time $t = t_j$, see Fig.4.

3. Data segmentation. See next subsection for more details.

4. Fit the function $P(f, t|A_0, \lambda_t, Q_{sys}, f_{sys})$, Eq. (6), to the experimental value to obtain the parameters A_0, λ_t, Q_{sys}, and f_{sys}.

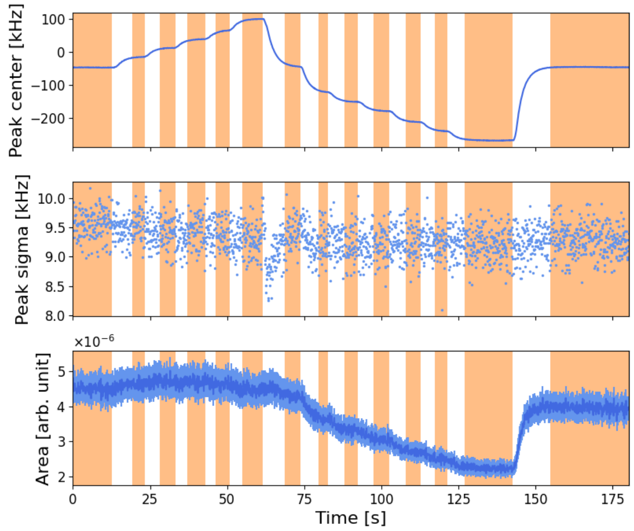

Fig. 4. Time evolution of the peak of $^{56}Fe^{26+}$ ions near 242.33 MHz (harmonic number $h = 616$): center frequency (top), peak width (middle), and peak area (bottom). At around 63 seconds, when the center frequency of the harmonic changed abruptly, the peak width is as well affected . Therefore, we only utilized the 14 data segments when the center frequency were stable, as indicated by the orange regions.

5. Implement the values of Q_{sys} and f_{sys} into Eq. (4) to obtain the AFC curve of the detection system. These two parameters are independent of the ion beam and can be used throughout the experiment if the detector setting were fixed.

B. Error estimation of Q_{sys} and f_{sys}

The function $P(f, t|A_0, \lambda_t, Q_{sys}, f_{sys})$ in Eq. (5) is a bivariate nonlinear function. In the fitting procedure, the task is to find the optimized combination of parameters that make the following objective function reach minima:

$$S = \sum_j \sum_i \left(P^{exp}_{i,j} - A_0 e^{-\lambda_t t_j} \left(1 + Q_{sys}^2 \left(\frac{f_i}{f_{sys}} - \frac{f_{sys}}{f_i}\right)^2\right)^{-1}\right)^2, \tag{7}$$

Although the processing steps appear straightforward, numerous challenges remain. These include:

a. Data segmentation. It is important to accurately determine A_0 in Eq.7. During measurement, we adjusted the electron cooling 13 times. Fig.4 illustrates the changes in the center frequency, width and area (i.e. average ion power) of the ion peaks of the 616th harmonic. Upon completion of the electron cooling adjustment, the center frequency as well as the peak width fluctuates significantly. Within a few seconds, the velocity of the ions reach equilibrium, and the peak position stabilized. Consequently, the data were filtered into 14 seg-

ments indicated by the orange regions in Fig.4 where the equilibrium was reached. Instead of using single initial peak area parameter A_0, fourteen independent initial peak area $A_{0,k}(k = 1, 2, ..., 14)$ are assigned to the corresponding data segments. The timing t_j in each data segment were also readjusted accordingly to the new stating points so that $A_{0,k}$ is encountered at $t_{k,j} = 0$. Hence, the objective function of the fitting is altered to:

$$S = \sum_{k=1}^{14}\sum_{j=1}^{n_k}\sum_{i=1}^{N_k}\left(P_{k,j,i}^{exp} - A_{0,k}e^{-\lambda_t t_{k,j}}\left(1 + Q_{sys}^2\left(\frac{f_{k,i}}{f_{sys}} - \frac{f_{sys}}{f_{k,i}}\right)^2\right)^{-1}\right)^2, \tag{8}$$

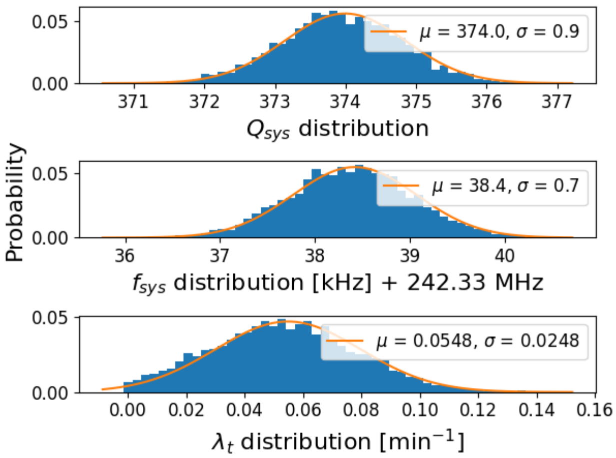

Fig. 5. Parameter distributions obtained by Monte Carlo calculations: from top to bottom, the probability distributions of parameters Q_{sys}, f_{sys}, and λ_t. The mean and variance of all the parameters are calculated using the Gaussian distribution with mean value μ and sigma value σ.

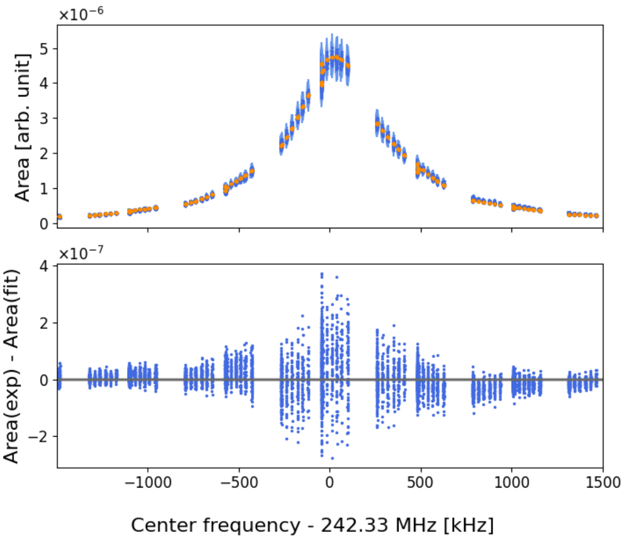

Fig. 6. Top panel: comparison between the measured peak area (blue dots) and the calculated peak area (orange dots) using fitted AFC function of the CSRe Schottky detector system. There are some sudden drop of the data points, due to twice passing through the frequency area during the measurements, see Fig. 3. Bottom panel: the differences between the measured and fitted peak area.

where N_k represents the number of measured harmonics in the spectrum of each data segment.

b. Monte Carlo calculations are used to estimate the value and error of the fitting parameters: Q_{sys}, f_{sys}, λ_t and $A_{0,k}(k = 1, 2, ..., 14)$. Part of the results is shown in Fig. 5. The estimated value and error of each parameter are the mean and variance of its distribution, respectively.

C. Fitting results of the AFC function

The characteristic parameter values of the AFC of the CSRe Schottky system are determined to be $Q_{sys} = 374.0 \pm 0.9$ and resonant frequency $f_{sys} = 242.3684 \pm 0.0007$ MHz, as illustrated in Fig. 5. The resultant AFC curve is shown as the orange dots in Fig. 6. The fitting residuals are fairly uniformly distributed around zero, indicating a good estimation of the Q_{sys} and f_{sys}. Notably, due to significant power estimation errors for ion harmonics near the resonant frequency, larger residuals are evident in this region.

This Q value of the detection system is smaller than the Q value of the Schottky cavity itself, $Q_{cavity} = 496.8$ [8]. It is reasonable since other components in the system can reduce resonance. To achieve higher Q_{sys} and thus higher sensitivity of heavy ion detection, new Schottky resonant cavities without ceramic beam pipe are under construction at next-generation SRing facility [22]. It is foreseen that 4 times higher Q_{cavity} will be reached for the stainless steel cavity and 20 times for the copper coated cavity[23].

IV. APPLICATION OF THE AFC FUNCTION TO THE STORAGE LIFETIME MEASUREMENT OF ^{56}FE^{26+} IONS AT DIFFERENT ENERGIES

After the AFC curve of the Schottky detector system was determined, we have conducted the storage lifetime measurements of fully ionized ^{56}Fe^{26+} ions under the same detector setting. The decay constant of the ions are determined from the normalized peak area in the revolution frequency spectrum and the storage half life can be converted from decay constant by $T_{1/2} = ln(2)/\lambda$. The results are summarized in Table 1.

Two beam energy settings were used and the electron-cooling had only ON or OFF status. There was no voltage and current adjustments during ON status, which is different from the measurement procedure of the AFC determination. The first energy was set at 13.7 MeV/u, the same as setting of the AFC curve measurement. The measured decay constant of the electron-cooled ^{56}Fe^{26+} ions is $0.0476(1)$ min^{-1} which is consistent with $\lambda_t = 0.054(25)$ min^{-1} determined during the AFC determination measurement (see Fig. 5 c). It is evident in table 1 that the decay constant of the fully ionized ^{56}Fe^{26+} is smaller when the electron-cooling was switched off. This can be understood by the fact that the electron beam of the cooler introduces additional beam loss mechanism to the stored ion beam.

The decay constants at higher beam energy of 116.4 MeV/u is more than one order of magnitude smaller than the ones at 13.7 MeV/u. At the high energy, the decay constant decreased by another order of magnitude after the electron cooling was switched off. This indicated that, at this beam energy, the main contribution of ion loss is that caused by the electron cooling process. Assuming realistic parameters of the CSRe cooler (electron beam vertical temperature 0.5 eV, current 0.2 A, radius ~ 4 cm), vacuum ($\sim 10^{-10}$ mbar, see section IV B) and temperature 20°C) , the calculated theoretical decay constant agree fairly well with the the measured values both at high energy [24, 26–29] and low beam energy [24, 25] as shown in the last two columns of table 1.

The importance of applying the AFC curve in the lifetime measurement can be clearly demonstrated by the measurements set on the beam energy of 116.4 MeV/u. The subsequent sections utilize the findings from this setting to elucidate the indispensability of the AFC curve in lifetime measurements.

A. Correcting for sudden peak area changes

Figure 7 illustrates the Schottky spectrum of the electron-cooled ^{56}Fe^{26+} ion beam. By accident, the center frequency of the peak underwent five abrupt shifts as shown in Fig. 7(b). This directly resulted in a corresponding rapid change and restoration of the peak center frequency and peak area within 2 minutes, which is derived from the spectra without AFC-normalisation as depicted in Fig. 7(b) and (c). Excluding the data during these perturbation periods, the ion storage lifetime is determined to be $144(8)$ min with a reduced data set.

Table 1. Measured storage lifetimes (respented by decay constant $\lambda = ln2/T_{1/2}$) of the ^{56}Fe^{26+} ions in the CSRe operated under the internal target mode ($\gamma_t = 2.457$) [17]. The measured decay constants of ion numbers in the ring λ_s(Exp) were compared to the calculated λ_s(Theory) [24, 26–29], where realistic parameters of the CSRe cooler (electron beam vertical temperature 0.5 eV, current 0.2 A, radius ~ 4 cm) and vacuum ($\sim 10^{-10}$mBar, 20°C) were utilized in the computation. For ions with energy of 13.7 MeV/u, no suitable theoretical formula was found to estimate their lifetime, and only the upper and lower bounds of the lifetime were given based on References [24, 25].

ECooler Status	Energy [MeV/u]	γ	λ_s(Exp) [min^{-1}]	λ_s(Theory) [min^{-1}]
ON	116.4	1.125	0.00685(9)	0.00648
OFF			0.00051(4)	0.0003
ON	13.7	1.027	0.0476(1)	0.03066< λ_s <0.6968
OFF			0.035(2)	0.0178< λ_s < 0.684

After the AFC curve is employed to normalize the ion peak area, as demonstrated in Fig. 7(d), the effects of the perturbations are mitigated. The normalized peak area follows the exponential decay trend, in despite of frequency shifts. This indicates that the swift frequency shifts haven't introduced additional loss of ions during the experiment. The ion storage lifetime derived from the normalized peak area is $145(2)$ min. This result is consistent with that obtained using a reduced dataset, but with enhanced precision. The observed five perturbations may be attributed to the sudden charging and discharging of high voltage power supply of the electron cooler. In similar situations of frequency drifts, the AFC curve is key for correctly and precisely determine the storage lifetime of the stored ions.

B. Effective vacuum experienced by the stored ions

After the electron cooling is turned off, the energy loss of the beam caused by the collisions between ions and residual gas can not be compensated any more. As a result, the momentum of the beam ions deceases and the momentum spread increases gradually. The absolute rate of frequency change df/dt is proportional to the effective vacuum experienced by the stored ions. Using the AFC normalized spectrum, the peak shape can be restored and peak center frequency can be determined with better precision. The effective vacuum can be derived from the obtained df/dt and the storage life time of the ion can be obtained from the normalized peak area decreasing as a function of storage time.

As shown in Fig. 8, upon deactivating the electron cooling (approximately at 0.8 seconds) , the ion momentum spread began to increase and the ion peak's center frequency drifts towards the lower frequency. From the measured AFC-curve in Fig. 6, it is clear that the frequency drifts towards where the maximum system AFC is located. That is why the peak area, which is deduced from the spectra before AFC-normalization, result in an increasing trend over time as shown in Fig. 8 (c). From the normalized peak area, the decreasing trend is restored and storage lifetime is determined to be $1954(139)$ min.

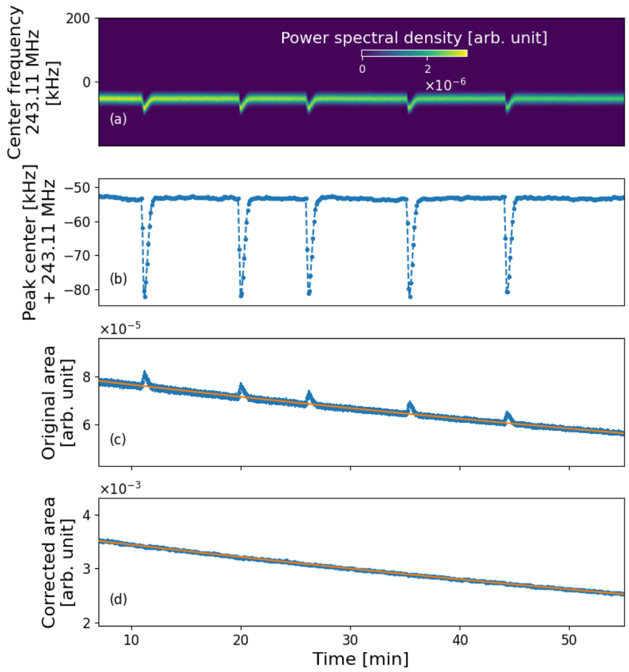

Fig. 7. (a) Time-resolved Schottky spectrum of $^{56}Fe^{26+}$ at beam energy of 116 MeV/u with electron-cooling switched on. The horizontal axis is the observation time, the vertical axis representing frequency, and the power density being distinguished by color. The frequency resolution is 0.12 kHz/channel and the time resolution is 6.39 seconds/bin. The evolution of the peak center frequency (b), peak area before (c) and after (d) AFC-normalization as a function of time are also shown. It can be clearly seen that there are 5 jumps during the acquisition period.

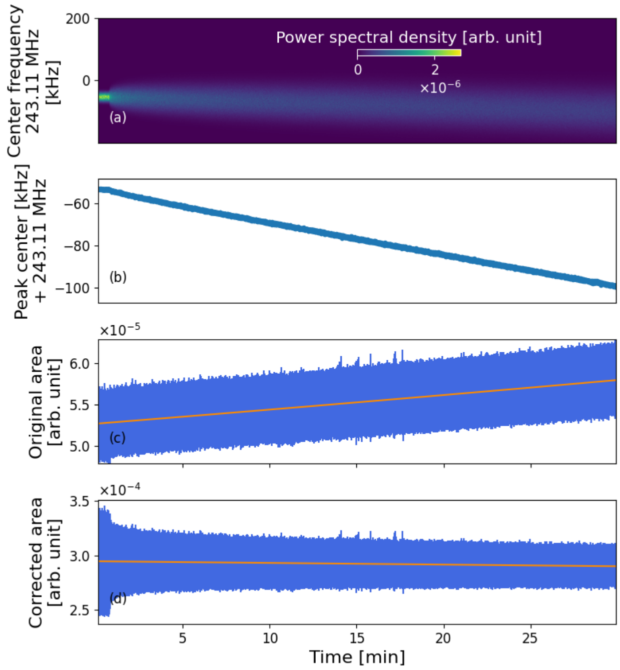

Fig. 8. (a) Time-resolved Schottky spectrum of $^{56}Fe^{26+}$ at beam energy of 116 MeV/u. The electron-cooling is switched off at around 0.8 second. The evolution of (b) peak center frequency, peak area before (c) and after (d) AFC-normalization as a function of time are also shown. It is evident that after the electron cooler was switched off, the frequency spread increased and the center frequency gradually drifted toward lower frequencies. The frequency resolution is 0.24 kHz/channel and the time resulution is 0.32 seconds/bin.

From the rate of the peak center frequency change observed in Fig. 8(b), $df/dt \approx 23$ Hz/s, the ion energy loss rate dE/dt can be deduced using formulae $df/f = (\gamma^{-2} - \gamma_t{}^{-2})dE/E$ where $\gamma_t = 2.457$ and γ is the Lorentz factor of the ions. This calculation yielded a value of $dE/dt \approx 1.89$ keV/s. Assuming a temperature of 20°C and the measured composition of the residual gas [30], the equivalent vacuum of the CSRe was estimated to be approximately 2×10^{-10} mbar. This value resprents the effective vacumm expercienced by the stored $^{56}Fe^{26+}$ ions. In total, 11 ultra-high vacuum gauge was used in the experiment and they were distributed evenly along the CSRe ring. Most of the gauge reading is on the level of 10^{-11} mbar except the one near the internal target area reading $\approx 4 \times 10^{-10}$ mbar. The effective vacuum feels by the stored ions agreed with the vacuum gauge readings.

With the derived effective vacuum of 2×10^{-10} mbar, the theoretical beam loss rate due to ion-gas collision were calculated to be 3×10^{-4} min^{-1}, corresponding to a storage lifetime of about 3333 min. However, current theoretical studies on ion storage lifetimes involve a wide range and complexity of reactions and factors, and the theoretical estimates are only informative on the order of magnitude. The experimental results we obtained are of the same order of magnitude as the theoretical estimates, which confirms the reliability of our methodolgy and the stability of the current CSRe operation.

V. SUMMARY AND OUTLOOK

In this work, we developed a novel method to calibrate the amplitude-frequency characteristic (AFC) curve of the Schottky detection system at the CSRe storage ring. Following calibration, there was a significant improvement in the accuracy of the peak position and the peak area determination in the revolution frequency spectra of the ions. The storage lifetimes of $^{56}Fe^{26+}$ ions were determined with high precision at 13.7 and 116.4 MeV/u, in despite of frequency shifts or frequency spreading increases occurred during the experiment. Additionally, when the electron cooling was switched off, the effective vacuum seen by the stored ions was deduced to be on the order of 10^{-10} mbar, consistent with the order of magnitude displayed by the vacuum gauge.

This method serves as a useful tool for storage ring Schottky frequency spectrum mass spectrometer to obtain accurate ion lifetimes. When electron cooling is enabled, the method can mitigate the negative effects of irregularities caused by electron cooling device instabilities. When electron cooling is disabled, residual gas collisions cause ion energy loss, leading to ion revolution frequency shifts. By applying the method developed in this paper, accurate and reliable lifetime

results can be obtained. One focus of next-generation Schottky mass spectrometry is the simultaneous measurement of masses and lifetimes of short-lived ions. Disabling electron cooling can extend the applicability of the technique from the minute range to the tens of milliseconds range [31]. In this context, the correction method presented in this work can play a significant role. The method developed at the CSRe can easily be adapted at other Storage ring facilities, such as the ESR and the CR at GSI (FAIR) in Darmstadt, Germany and the R3-Ring at RIKEN in Saitama, Japan.

For the next generation storage rings, such as the HIAF-SRing in Huizhou [32], new Schottky detectors with higher sensitivity and transverse position sensitivity will be built. The methodology developed in this paper will serve as foundational components for the advancement of Schottky mass spectrometry, which is anticipated to be pivotal in the discovery and precise measurement of exotic nuclei in future endeavors [33].

ACKNOWLEDGEMENT

We would like to extend our gratitude to Prof. F. Caspers for his insightful comments on measurement principles, which greatly improved the manuscript. Suggestions on vacuum calculation from Dr. Yingli Xue and Dr. Cheng Luo are greatly acknowledged.

---

[1] F. G. Kondev, M. Wang, W. J. Huang, S. Naimi, and G. Audi, The NUBASE2020 evaluation of nuclear physics properties. Chinese Phys. C **45**(3), 03001 (2021). doi: 10.1088/1674-1137/abddae
[2] X. W. Xia, Y. Lim, P. W. Zhao, *et al.*, The limits of the nuclear landscape explored by the relativistic continuum HartreeBogoliubov theory. Atom. Data Nucl. Data **121–122**, 1–215 (2018). doi: 10.1016/j.adt.2017.09.001
[3] Léo Neufcourt, Yuchen Cao, Samuel A. Giuliani, *et al.*, Quantified limits of the nuclear landscape. Phys. Rev. C, **101**(4), 044307 (2020). doi: 10.1103/PhysRevC.101.044307
[4] Y.H. Zhang, Yu.A. Litvinov, U. Uesaka, and H.S. Xu. Storage ring mass spectrometry of nuclear stucture and astrophysics research. Phys. Scripta, **91**, 073002 (2016). doi: 10.1088/0031-8949/91/7/073002
[5] Yu. A. Litvinov, F. Bosch. Beta decay of highly charged ions. Rep. Prog. Phys., **74**(1), 016301 (2011). 10.1088/0034-4885/74/1/016301
[6] Yu. A. Litvinov, S. Bishop, K. Blaum,*et al.*, Nuclear physics experiments with ion storage rings. Nucl. Instr. Meth. Phys. Res. B., **317**, 603–616 (2013). doi: 10.1016/j.nimb.2013.07.025
[7] B. Franzke, H. Geissel, G. Münzenberg. Mass and lifetime measurements of exotic nuclei in storage rings. Mass Spectrom. Rev., **27**(5), 428-469 (2008). 00090. doi: 10.1002/mas.20173
[8] J.X. Wu, Y.D. Zang, F. Nolden, *et al.*, Performance of the resonant Schottky pickup at CSRe. Nucl. Instr. Meth. Phys. Res. B., **317**, 623–628 (2013) doi: 10.1016/j.nimb.2013.08.017
[9] K. Beckert, S. Cocher, B. Franzke, and U. Schaaf. The ESR schottky-dagnosis-system. in *Proceedings of 2nd European Particle and Accelerator Conference*. 2nd European Particle and Accelerator Conference, Nice, France, 1990. p 777
[10] Z. Du, P.L. He, G.Y. Zhu, *et al.*, Development of a diagonal-cut type beam position monitor for the booster ring in the high intensity heavy-ion accelerator facility project. Rev. Sci. Instrum., **93**(4), 043306 (2022). doi: 10.1063/5.0083344
[11] F. Nolden, P. Hülsmann, Yu. A. Litvinov, *et al.*, A fast and sensitive resonant Schottky pick-up for heavy ion storage rings. Nucl. Instr. Meth. Phys. Res. A., **659**(1), 69–77 (2011). doi: 10.1016/j.nima.2011.06.058
[12] F. Suzaki, Y. Abe, A. Ozawa, *et al.*, A resonant Schottky pick-up for Rare-RI Ring at RIKEN. Phys. Scripta, **T166**, 014059 (2015). doi: 10.1088/0031-8949/2015/T166/014059
[13] M. S. Sanjari, D. Dmytriiev, Yu. A. Litvinov, *et al.*, A 410 MHz resonant cavity pickup for heavy ion storage rings. Rev. Sci. Instrum., **91**(8), 083302 (2020). doi: 10.1063/5.0009094
[14] P. Kienle, F. Bosch, P. Bühler, *et al.*, High-resolution measurement of the time-modulated orbital electron capture and of the β^+ decay of hydrogen-like $^{142}\mathrm{Pm}^{60+}$ ions. Phys. Lett. B, **726**(4–5), 638–645 (2013). doi: 10.1016/j.physletb.2013.09.033
[15] B. Franzke. The heavy ion storage and cooler ring project ESR at GSI. Nucl. Instr. Meth. Phys. Res. B, **24–25**, 18–25 (1987). doi: 10.1016/0168-583X(87)90583-0
[16] A. Ozawa, T. Uesaka, M. Wakasugi. The rare-RI ring. Prog. Theor. Exp. Phys., **2012**, 03C0009 (2012). doi: 10.1093/ptep/pts060
[17] J.W. Xia, W.L. Zhan, B.W. Wei, *et al.*, The heavy ion cooler-storage-ring project (HIRFL-CSR) at Lanzhou. Nucl. Instr. Meth. Phys. Res. A, **488**(1–2), 11-25 (2002). doi: 10.1016/S0168-9002(02)00475-8
[18] Q. Wang, X.L. Yan, X.C. Chen, *et al.*, Spectral baseline estimation using penalized least squares with weights derived from the Bayesian method. Nucl. Sci. Tech, **33**(11), 148 (2022). doi: 10.1007/s41365-022-01132-9
[19] G. Y. Qiu, *Circuit*, 5th edn. (Higher Education Press, Beijing, 2006).
[20] X. X. Yang, Z. X. Yi, *Fundamentals of Microwave Technology*, 3rd edn. (Tsinghua University Press, Beijing, 2021).
[21] P.B. Wilson. Introduction to wakefields and wake potentials. AIP Conf. Proc., **184**, 525-569 (1989).
[22] B. Wu, J.C. Yang, J.W. Xia, *et al.*, The design of the Spectrometer Ring at the HIAF. Nucl. Instr. Meth. Phys. Res. A, **881**, 27–35 (2018). doi: 10.1016/j.nima.2017.08.017
[23] G.Y. Zhu, Private communication, August 2024.
[24] I. S. Dmitriev, V. P. Zaikov, E. A. Kralkina, *et al.*, On the target thickness to attain equilibrium charge distribution in a beam of fast ions. Nucl. Instr. Meth. Phys. Res. B, **14**(4–6), 515–526 (1986). doi: 10.1016/0168-583X(86)90148-5
[25] A. S. Schlacher, J. W. Stearns, W. G. Graham, *et al.*, Electron capture for fast highly charged ions in gas targets: an empirical scaling rule. Phys. Rev. A, **27**(11), 3372(R) (1983). doi: 10.1103/PhysRevA.27.3372
[26] B. Franzke. Interaction of stored ion beams with the residual gas. in *CAS - CERN Accelerator School: fourth advanced accelerator physics course*. CAS - CERN Accelerator School: fourth advanced accelerator physics course, Dourdan, France,

1992. pp. 100-119 doi: 10.5170/CERN-1992-001.100

[27] H. Poth. Electron cooling: Theory, experiment, application. Phys. Rep., **196**(3–4), 135-297 (1990). doi: 10.1016/0370-1573(90)90040-9

[28] I.Yu. Tolstikhina, V.P. Shevelko. Collision processes involving heavy many-electron ions interacting with neutral atoms. Phys. Usp, **56**(3), 213-242 (2013). doi: 10.3367/UFNe.0183.201303a.0225

[29] X. Y. Zhang. Master Thesis, University of Chinese Academy of Sciences, 2005.

[30] H.B. Wang, Phd. Thesis, University of Chinese Academy of Sciences, 2017.

[31] Yu.A. Litvinov, R.J. Chen. Radioactive decays of stored highly charged ions. Eur. Phys. J. A, **59**(5), 102 (2023). doi: 10.1140/epja/s10050-023-00978-w

[32] J.C. Yang, J.W. Xia, G.Q. Xiao, *et al*., High intensity heavy ion accelerator facility (HIAF) in China. Nucl. Instr. Meth. Phys. Res. B, **317**, 263–265 (2013). doi: 10.1016/j.nimb.2013.08.046

[33] T. Yamaguchi, H. Koura, Yu.A. Litvinov, M. Wang. Masses of exotic nuclei. Prog. Part. and Nucl. Phys., **120**, 103882 (2021). 10.1016/j.ppnp.2021.103882